JOURNAL OF GEOPHYSICAL RESEARCH, VOL. 104, NO. E11, PAGES 27,067–27,077, NOVEMBER 25, 1999

Raman spectroscopic characterization of a highly weathered basalt: Igneous mineralogy, alteration products, and a microorganism

Alian Wang, Bradley L. Jolliff, and Larry A. Haskin

Department of Earth and Planetary Sciences and McDonnell Center for the Space Sciences, Washington University, St. Louis, Missouri

Abstract. On-surface identification of minerals on Mars is likely to depend mainly on observations of rocks and soils as found, without access to fresh surfaces or other sample preparation. Both the original mineralogy of rocks and their alteration mineralogy will be important. To determine the capability of Raman spectroscopy to provide good mineralogical characterization of an altered igneous rock such as might be encountered on Mars, we have analyzed the heavily weathered, exterior surface of a cobble of Keweenawan basalt and compared the results with those from a roughly cut, unpolished interior surface, using a Raman point-counting method. Despite ubiquitous hematite, a strong Raman scatterer, and despite considerable alteration, original igneous plagioclase and pyroxene were identified and their approximate proportions determined from point-counting traverses on the original surface of the rock. Saponite, an alteration product, was easily identified on the freshly cut surface but could only occasionally be identified on the weathered surface, where saponite-rich areas were highly photoluminescent. Amygdular fill gave strong spectra of calcite and thomsonite (a zeolite). Tiny, sparse crustose lichen gave clear spectra of their waxy organic coating. On the basis of the surface Raman spectra alone, the rock could be identified as a mafic rock, probably basaltic, that was hydrothermally altered in an oxidizing environment at a temperature between ~250 and ~350°C.

1. Introduction

Rover- or lander-based Raman spectroscopy can provide definitive, detailed, in situ mineral characterization and rock identification on planetary surfaces. Past studies [*Wang et al.*, 1995; *Haskin et al.*, 1997; *Wang et al.*, 1998a] have shown that Raman spectroscopy offers unambiguous identification of minerals that contain oxy-anion groups (silicates, carbonates, sulfates, phosphates, etc.) or that consist of oxides, hydroxides, sulfides, etc. An early application could be to Martian rocks and soils during the Mars Surveyor missions in the next 10 years.

The red color typical of Martian surface materials suggests that many of these materials have been altered to oxides or oxyhydroxides of ferric iron or have become coated with them [e.g., *Bell et al.*, 1995]. Hematite has been identified using the thermal emission spectrometer (TES) on the Mars Global Surveyor [*Lane et al.*, 1999], and spectral characteristics of rocks at the Mars Pathfinder site suggest the presence of maghemite or ferrihydrite in altered rock surfaces [*McSween et al.*, 1999]. Thus it is necessary to determine what can be learned from altered rocks or rock surfaces by using Raman spectroscopic techniques. In particular, can rock types be determined despite alteration? Can environments of alteration be determined by mineralogical analysis? Can the roles of water and atmospheric components in the formation and alteration of Martian rocks and soils be discovered by automated on-surface analysis? Is there evidence for reduced inorganic carbon and organic compounds? Answering those questions requires knowledge of the detection limit of minerals and carbonaceous materials, especially when they occur as mixtures or are rare in or on rocks. We may anticipate that modal information obtained from the surface of a coated or weathered rock will require careful interpretation.

Our past work has shown that igneous minerals can readily be identified [*Wang et al.*, 1995], and their proportions quantified [*Haskin et al.*, 1997]. This includes a sample of an actual Martian rock, the Zagami meteorite [*Wang et al.*, 1999a]. All of those analyses were done on fresh surfaces. Preliminary study of a varnish-coated basalt [*Israel et al.*, 1997] showed that minerals within the varnish coating itself could be identified and where the varnish was thin or absent, the original igneous minerals could be identified. The type of varnish coating on rocks from terrestrial desert environments is biologically derived, however, and not necessarily a good analog for Martian rocks. The results from the recent Pathfinder-Sojourner alpha proton X-ray spectrometer (APXS) major-element chemical analyses [*Reider et al.*, 1997] can be interpreted as indicating that dust partially coated the surfaces of most of the rocks analyzed. Images showed areas of rock with sand-blasted textures, indicating that some rock surfaces may be relatively free from any type of coating or to have very thin coatings [*McSween et al.*, 1999]. So, some access to fresh rock surfaces, either as dust-poor ventifacts or as spaces between dust coatings, can be expected. Nevertheless, the possibility remains that in some locations Martian rocks may have been considerably altered by hydrothermal, aqueous sedimentary, or surface weathering processes. To simulate what might be learned from an in situ Raman spectrometer examining altered Martian basalt, we have examined the weathered surface of an ancient terrestrial basalt to learn what can be determined by such an analysis

Copyright 1999 by the American Geophysical Union.

Paper number 1999JE001071.

0148-0227/99/1999JE001071$09.00

without producing a fresh specimen. In general appearance, the rock surface is relatively smooth but with considerable fine-scale relief, and is brick-red in color with spots and amygdular fill of white to tan material. Also for this study, we configured our laboratory Raman spectrometer to operate in a point-count mode [*Haskin et al.*, 1997] with a long working distance objective, very similar to the Athena Raman system currently under development for the Mars Surveyor Program.

2. Samples and Experiment

The rock specimen examined in this study is a large (football-sized) cobble of a strongly altered basalt from the 1100 Ma Keweenawan North Shore Volcanic Group [*Brannon*, 1984], collected along the north shore of Lake Superior, northeastern Minnesota. This sample, designated AKB-1 (altered Keweenawan basalt [*Morris et al.*, 1998]) was selected for study because it was altered extensively by hydrothermal and low-temperature processes, yet it still retains evidence of its igneous mineralogy and composition. Two types of surfaces of this rock were studied. One was the heavily weathered exterior surface (Plate1a), with local surface relief of several millimeters. The second was a roughly cut, flat, unpolished surface (Plate1b). Examination of these two surfaces with the Raman spectrometer enabled a comparison of results from the weathered, unprepared surface with a freshly exposed surface.

The rock consists of a fine-grained, reddish, altered basaltic groundmass containing small (several millimeters) ovoids of a soft, grayish green clay mineral, possibly an alteration product of a primary phenocrystic phase (probably olivine), and coarse (centimeter size) light-colored amygdules filled by zeolite and calcite. The groundmass has textural domains ranging from relict subophitic to intergranular to radiate (Figure 1), consisting mainly of laths of partially to strongly altered feldspar forming a nearly complete, interconnected network, and interstitial pyroxene mesostasis. These saponite-filled ovoids therefore may be pseudomorphs after magnesian olivine phenocrysts. Some of these ovoids contain calcite and zeolite in addition to saponite.

Electron microprobe analysis of pyroxene yields a high-Ca composition of $En_{37-38}Fs_{17-20}Wo_{43-45}$, taking all Fe as Fe^{2+}, but including a significant Al component ($Al_2O_3 \sim 3$–4 wt%). The identification of Mg-rich smectite (saponite) is confirmed (SiO_2 = 43 wt%, MgO = 26 %, Al_2O_3 = 9 %, FeO = 2 %, and CaO = 2.2 %). Analysis of plagioclase reveals a range from Ab 84 to Ab 97, reflecting albitization, and the Ca/Na ratio of altered more calcic parts of grains, if unchanged by alteration, suggests an original plagioclase composition of about An 50 to An 60.

Samples analyzed by Raman spectroscopy were prepared in several different ways. The original football-sized, oblong rock was sawn and slabbed using a large diamond-impregnated metal blade and tap water for lubrication and cooling. Rock fragments containing the exterior, weathered surface were rinsed ultrasonically in deionized water. Interior sections from the slab were ground gently to remove saw marks. These sections were also rinsed in deionized water prior to Raman analysis. Thin sections prepared from the slab were bonded with super glue.

Automated Raman spectral point-counting measurements were made either along linear traverses or at points on a rectangular grid on both rock surfaces. Additional Raman measurements were made on selected locations and within areas of mesostasis. The lines and rectangles shown on Plates1a and 1b indicate the locations of the linear and grid traverses along which Raman measurements were taken.

The instrument used for this study is a HoloLab 5000 (Kaiser Optical Systems, Inc.) Raman spectrometer. The excitation source is the 632.8 nm line from a He-Ne laser. The laser beam is carried by optical fiber to the sampling probe head, which directs it toward the sample surface through a microscope, which in turn, collects the backscattered radiation. A second optical fiber carries the backscattered radiation to the spectrograph. The spectrograph

gether, this means that the sampled volumes in our Raman experiments are typically <100 μm in diameter, and likely significantly less for some of the spectra taken. These complications are described in more detail by *Haskin et al.* [1997] and by *Wang* [1999].

3. Raman Measurements and Results

3.1. Phase Identification in the Rock Matrix and Amygdules

We first identified the mineral phases exposed on both the original heavily weathered exterior surface and the roughly cut, flat, unpolished surface of the rock by examining selected mineral grains of different morphologies. Figure 2 shows typical Raman spectra of the mineral phases obtained in this way.

3.1.1. Matrix minerals. The main mineral phases found in the dark red matrix of this rock are hematite (alpha-Fe_2O_3), pyroxene, plagioclase, and saponite (Figure 2a). Minor and trace minerals observed include K-feldspar, quartz, and anatase (a polymorph of TiO_2) (Figure 2b).

The dominant matrix mineral seen in the spectra is hematite (Figure 3a), which is responsible for the reddish color of the rock matrix. Pure, well-crystallized hematite yields sharp major Raman peaks near 1322, 612, 411, 294, and 227 cm^{-1} [*Wang et al.*, 1998b]. The peak positions of hematite in this rock vary from location to location within the matrix. The most obvious variations are the position of a sharp doublet near 294 and 227 cm^{-1} and the intensity of this doublet relative to other peaks. In most hematite spectra the peak positions of this doublet varied and occurred several wavenumbers below the expected value, ranging downward to as low as 274 and 214 cm^{-1}. For some extreme cases this doublet was the only observed feature in the spectra. This suggests a considerable variation in the crystallinity and grain size of the hematite in this rock.

Two types of pyroxene spectra were observed (Figure 2a). Characteristic Raman spectra of pyroxene were obtained in a few locations but with very low signal-to-noise ratio. These spectra were obtained from the rare, relict pyroxene grains as observed in thin section. The best three of these have peak positions suggesting an Mg' [=molar $Mg^{2+}/(Mg^{2+} + Fe^{2+})$] value of ~0.4 – 0.5, a little lower than the ~0.6 obtained from the relict grains analyzed by electron microprobe (EMP). It is uncertain whether these values of Mg' represent the pre-alteration pyroxene composition (see *Wang et al.* [1999b] for information on the pyroxene calibration).

The more common type of pyroxene-like spectrum was found in conjunction with the spectrum of hematite (Figure 2a) and is presumably a consequence of the alteration of pyroxene leading to hematite. Backscattered-electron imaging shows that pyroxene grains are invariably coated (or altered on their Fe-rich rims) by hematite (Figure 1d). These pyroxene spectra showed only one clear Raman peak, a strong peak above 660 cm^{-1}, produced by the symmetrical stretching vibration of Si-O_b-Si bonding (where O_b is bridging oxygen) in $[Si_2O_6]_n$ chains in the pyroxene structure. The other major Raman peak of normal pyroxene (near 1000 cm^{-1}), which would be produced by the symmetric stretching vibration of Si-O_{nb} bonds (where O_{nb} is nonbridging oxygen) in SiO_4 tetrahedra, was rarely observed or was very weak in these spectra. In general, a reduction in the fraction of oxygens that are nonbridging (e.g., polymerization) reduces the intensity of the peak near 1000 cm^{-1} and causes a shift of the peak near 670 cm^{-1} toward higher wavenumbers [*Wang et al.*, 1994]. This reduction in the fraction of nonbridging oxygens is consistent with transmission electron microscope (TEM) studies showing that pyroxene alters to hydrous pyriboles (amphiboles and wider-chain silicates), to sheet silicates, and to pyroxenoids [*Buseck et al.*, 1982]. The observed peak position (661 to 668 cm^{-1}) is too low to suggest a sheet silicate (>680 cm^{-1}) and the lack of the peak near 1000 cm^{-1} rules out pyroxenoids. The 661 – 668 cm^{-1} peak is in the range expected for pyriboles, although no OH peak was observed that would confirm this assignment. The OH peak could be difficult to detect in this fine-grained matrix, however. For the purpose of phase identification (but not pyroxene alteration) in this study, we will use the term "pyroxene" to specify the mineral observed in both types of spectra.

Plagioclase is the second most abundant matrix mineral of this rock (Figure 2a). Almost all plagioclase spectra are mixed with peaks from hematite and commonly pyroxene, both of which are stronger Raman scatterers than plagioclase. The major Raman spectral feature of plagioclase is a doublet in the 460-520 cm^{-1} region, assigned to the vibrational mode of T-O_b-T (T = Si or Al) units by previous studies [*Sharma et al.*, 1983]. In the spectra obtained from this rock, the exact positions of these two peaks vary within a narrow range, from 503 to 510 cm^{-1} for the first peak, and from 475 to 480 cm^{-1} for the second peak. This variation, accompanied by variations in peak widths, suggests the existence of plagioclase of different albite-anorthite proportions and a decrease in the regularity of the plagioclase structure as a consequence of alteration. Based on petrographic observation and electron microprobe analysis, both are possible. Further Raman study is needed to learn the relationship between Raman features and structural and compositional characteristics of plagioclase. In several rare cases, the major peak was found near 513 cm^{-1}, and a triplet instead of a doublet appeared in that region (Figure 2b). Although the spectral pattern is still characteristic of feldspar, it is more characteristic of K-feldspar than of plagioclase.

Grayish green saponite occurs as clots and ovoids scattered throughout the fine-grained matrix. Saponite has its main Raman peaks near 3680, 3420, 680, 355, 295, and 190 cm^{-1} (Figure 2a). It shows only a weak feature in the 1000 cm^{-1} region of the spectrum. The general pattern of its spectrum is that of a sheet-silicate mineral with a ratio of O_b/Si >3. The main peak near 680 cm^{-1} is produced by the vibration of linked TO_4 (T = Si or Al) tetrahedra in $[Al_xSi_{4-x}O_{10}]_n$ tetrahedral layers. The position of that peak is characteristic of the tri-octahedral structure (in which bivalent cations fill all of the sites in the octahedral layers) and is lower than we have observed for minerals with di-octahedral structure. The sharp, intense peak near 3680 cm^{-1} could reasonably be assigned to the vibration of an OH group, and the broad band centered near 3420 cm^{-1} results from the vibrations of interlayer water molecules. In general, the structural features revealed by this Raman spectrum match very well with those of saponite $[Na_x(Mg_3(Al_xSi_{4-x}O_{10})(OH)_2 \cdot 4H_2O]$. A very similar spectrum was acquired from standard saponite sample SapCa-2 obtained from the American Clay Mineral Society.

3.1.2. Amygdule minerals. The minerals identified as amygdular fill were calcite and a zeolite (Figure 2c). The Raman spectral pattern of calcite is characterized by four major peaks at 1086, 713, 282, and 156 cm^{-1} [*Herman et al.*, 1987]. The first two peaks are produced by the symmetric stretching and bending vibrations of the CO_3^{2-} anionic group. The other two are the external vibrational modes that cause relative translations between the cations (Ca^{2+}) and the anionic groups. The exact positions of peaks in the carbonate spectra from the amygdules are characteristic of calcite ($CaCO_3$) and are readily distinguishable from those of magnesite ($MgCO_3$), siderite ($FeCO_3$), dolomite ($CaMg(CO_3)_2$), and aragonite, the other structural form of $CaCO_3$.

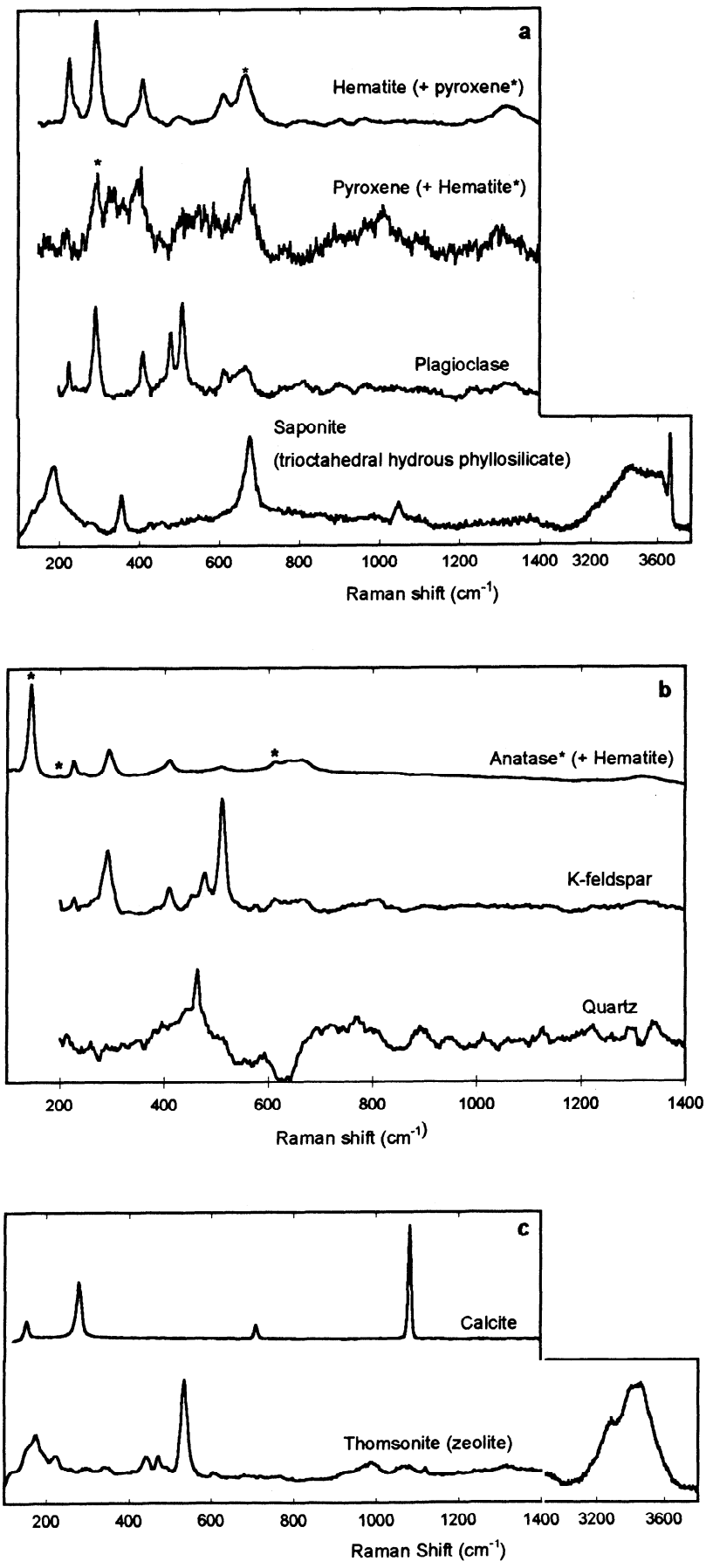

Figure 2. Typical Raman spectra of mineral phases found in rock AKB-1: (a) major mineral phases of the rock matrix, (b) minor mineral phases of the rock matrix, and (c) mineral phases of the amygdular fill.

The zeolite mineral is a thomsonite-gonnardite solid solution of the fibrous zeolite group and has a Raman spectrum very similar to that of the pure end-member thomsonite [*Wopenka et al.*, 1998] (ideal chemical formula $NaCa_2[(Al,Si)_5O_{10}]_2 \cdot 6H_2O$ [*Gottardi,* 1978]). Fibrous zeolites have a framework structure consisting of weakly cross-linked aluminosilicate chains along the *c* axis. The chain elements are rings of SiO_4 and AlO_4 tetrahedra. Elliptical cages or channels are present among the connected chains, within which H_2O molecules and large-diameter cations (e.g., Na^+, Ca^{++}) are located. Analysis by EMP yields formula proportions as follows: $Na_{1.0}Ca_{1.9}Al_{4.8}Si_{5.2}$ to $Na_{1.4}Ca_{1.4}Al_{4.2}Si_{5.8}$ (cf. ideal formula above). The Raman spectrum of thomsonite is characterized by peaks arising from the fundamental vibrational modes of the coupled TO_4 (T = Si or Al) tetrahedra and by peaks from the stretching and bending modes of H_2O molecules [*Wopenka et al.*, 1998]. These two groups of Raman peaks appear in the regions below 1200 cm^{-1} and between 3000–3800 cm^{-1}, respectively. The strongest Raman peak of thomsonite observed from the amygdule zeolite is located near 538 cm^{-1}, assigned in several previous studies [*Pechar and Rykl*, 1983; *Dutta and Del Braco*, 1985; *Dutta and Shieh*, 1986; *Dutta and Puri*, 1987] to the bending vibrational mode of the coupled T-O_b-T (T = Si or Al) units. The symmetrical and asymmetrical stretching modes of those units produce rather weak peaks near 700 cm^{-1} and 1040 cm^{-1}, and these could not be observed in most of the thomsonite spectra from this rock sample. The broad doublet near 3430 and 3280 cm^{-1} is from the stretching vibrations of OH bonds in water molecules. The number of peaks, the peak positions, and the peak widths depend on the local environmental symmetry of the water molecules, which is determined by the specific interconnections between the aluminosilicate chains in thomsonite. The spectral pattern of this region (as well as that of fundamental mode region) allowed us to distinguish thomsonite from the other fibrous zeolites, e.g., natrolite, mesolite, scolecite, gonnardite, and edingtonite [*Wopenka et al.*, 1998].

In many locations inside amygdules, thomsonite is either mixed with a third, highly photoluminescent phase (detected using a Raman imaging microscope, ChemIcon™ company), or it contains impurities that cause it to luminesce strongly. This photoluminescent background overwhelms the Raman peaks of thomsonite in these locations.

3.1.3. A Micro organism. Figure 3a shows a tiny crustose lichen, several of which are found on the original weathered rock surface. These lichens are ~180 μm in diameter, whitish yellow in color, and semi spherical in shape. Raman spectroscopic measurements on several of them yielded a consistent spectral pattern (Figure 3b). The most intense peaks are located near 2931, 839, 433, and 1727 cm^{-1}. The group of four sharp, intense Raman peaks near 2900 cm^{-1} is characteristic of vibrations of saturated C-H bonding (symmetric and anti symmetric stretching vibrations of CH_3 and CH_2). The sharp peak near 1727 cm^{-1} is from the C=O stretching vibration of a saturated aliphatic ester, which also

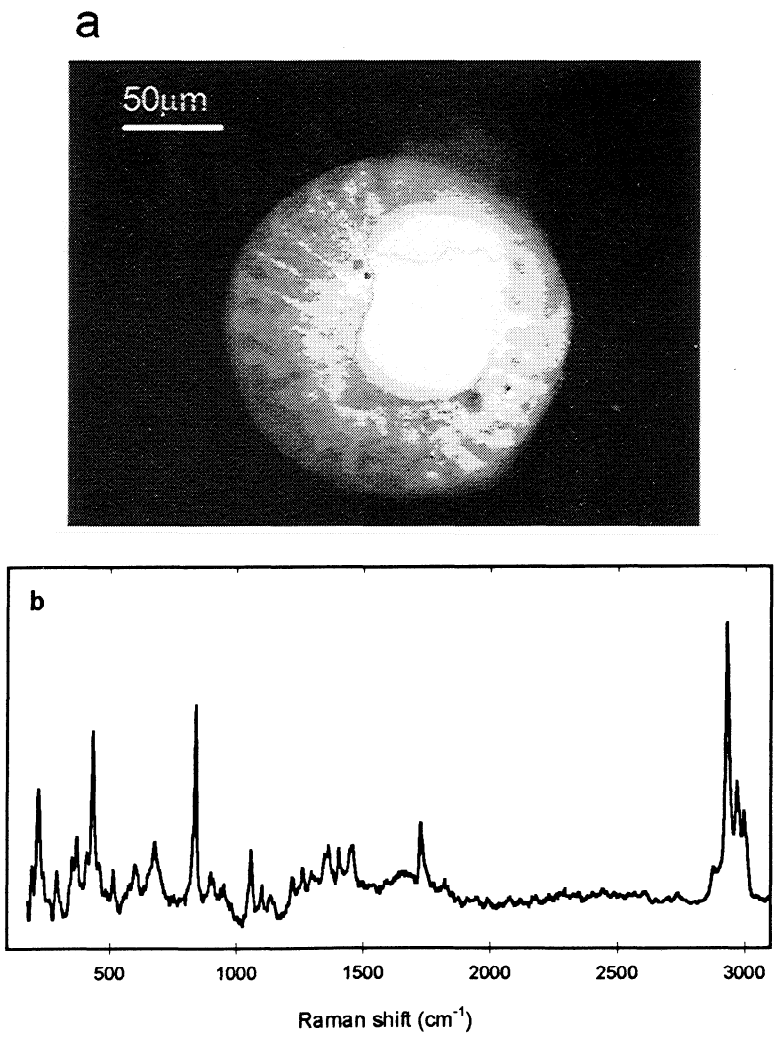

Figure 3. A crustose lichen on the weathered exterior surface of the rock: (a) top view of the lichen showing the inner shell and a partially broken outer shell and (b) typical Raman spectrum obtained from the crustose lichen.

shows a C-O stretching vibration near 1222 cm^{-1}. The group of peaks in the 1500 - 1300 cm^{-1} region arises from various vibrations of carbon-hydrogen bonds (deformation, twisting, etc.). The peaks at 839, 433, 1100, and 1058 cm^{-1} suggest a tertiary aliphatic branch. Many sharp and less intense peaks occur at lower wavenumbers. Overall, this spectral pattern is dominated by peaks from an ester of a long-chain aliphatic acid with a long-chain alcohol, one of which has a tertiary carbon, a type of material known to occur as waxy protective coatings exuded by some living organisms. A biological origin of the organic material can thus be inferred from the Raman spectrum.

3.2. Phase Distribution and Local Heterogeneity

Two sets of automated measurements were made on the original weathered rock surface along two linear traverses. The locations chosen for these traverses began in altered basalt matrix, crossed the major filled amygdule, and passed across more of the matrix on the opposite side (Plate 1a). The first of these measurements consisted of two parallel linear traverses, 32 points each, 100 μm between the lines, covering a linear distance of ~9 mm each. The second measurement, a single linear traverse of 60 points, also went from matrix to amygdular fill to matrix but crossed only a narrow tail of the large filled amygdule and covered a distance of 6 mm. The purpose of choosing these locations was to observe the transition in mineral phase distribution from matrix to amygdular fill and thus to simulate the identification minerals across a heterogeneous zone.

During a set of automated point-counting measurements, a fixed measurement time was selected for obtaining each spectrum (30 seconds each for the first traverse, 25 seconds each for the second), a fixed distance was taken for the intervals between measurement points (300 μm for the first and 100 μm for the second), and no focusing adjustment was done at individual measurement points. This last condition meant that, at most measurement points, the actual surface of the rock was above or below the focal plane of the laser beam. In order to determine the influence of laser defocusing (and thus of rock surface relief) on the quality of the spectra and the ability to identify the phases, an additional two sets of traverse measurements were made along the same traverse lines, and as close to the same measurement points as was feasible, but with adjustment of the focus for each measurement.

Plate 2 compares the phase identifications for second traverses, with and without focusing adjustment. The same basic information was obtained from the two types of experiment. The major minerals were identified at the same or nearby locations along the traverses. A spot by spot comparison for the matrix part of the rock shows a few discrepancies. Less plagioclase and, in some locations, less pyroxene were identified in the spectra taken without focusing adjustment. Also, more points showing high luminescence or yielding no significant spectral signals were encountered without focusing adjustment. Among the amygdular minerals, calcite (a strong Raman scatterer) was detected more often in the spectra taken without focusing adjustment, and the detection rate for minor mineral phases (e.g., anatase and quartz) was lower. One factor contributing to these differences is the unequal Raman cross sections for different mineral phases, such that the spectral peaks of the weaker Raman scatters (e.g., plagioclase and pyroxene relative to hematite) become less easily observed than those of stronger scatterers in spectra taken at a low signal-to-noise ratio. Another factor is the larger laser beam spot size at the rock surface when the beam is not in focus, which increases the chance that a mineral with a high local abundance or a large grain size will be detected and decreases the chance that grains of a rare mineral phase will be detected. Thus, although anatase and quartz are equally strong Raman scatters as calcite (anatase is even stronger), their much rarer occurrence in the amygdular fill and very small grain sizes are probably responsible for their less frequent identification in off-focus measurements compared to on-focus measurements at essentially the same sampling sites.

3.3. Mineral Modes of Rock Matrix

Two automated measurements were made on grid points located in rectangular matrix areas of both the heavily weathered exterior surface and the roughly cut, flat, unpolished surface. The grid areas were 2.4 × 4 mm (16 points per line × 7 lines, 150 × 600 μm as the fixed interval) for the weathered surface, and 11 mm × 4 mm (12 points per line × 9 lines, 1000 × 500 μm as the fixed intervals) for the freshly cut surface. The measurement times were 20 seconds and 30 seconds per spectrum. Plates 1a and 1b show the locations and the sizes of the two rectangular areas where these measurements were made. Both traverses were automated, i.e., without focusing adjustment beyond the first measurement point. From these experiments we are able to determine the difference in mineralogical composition and mode between the original, weathered surface and the fresh surface. Also, we would hope to obtain a mineral mode for the igneous materials of the matrix from direct analysis and from interpretation of their alteration products, and any differences between the mode of the fresh and weathered surfaces could affect that result.

Figure 4 shows pie diagrams of the mineral proportions found from the two grid traverses. The most frequently observed mineral was hematite. Most of the hematite spectra show the broad peak near 660 cm^{-1} of residual pyroxene. Only a trace of hematite-free pyroxene was found and then only in the freshly cut interior surface. Pyroxene was the second most frequently observed mineral, after hematite. The third most frequently observed mineral was plagioclase. The sums of hematite plus pyroxene plus plagioclase on the weathered exterior surface (89%) and on the roughly cut interior surface (87%) are almost equal. Spectra of saponite were obtained only from the freshly cut interior surface during the traverses and not from the weathered exterior surface. On the interior surface, saponite occurs as ovoidal mineral clots. Mineral clots of similar morphology occur on the weathered exterior surface, but these yielded saponite spectra only when individual, in-focus point checks were made, and these spectra have a high luminescent background. Instead of saponite, some 9 % of the 112 grid measurements from the weathered surface yielded high luminescence but no discernible spectral peaks. We know from the in-focus measurements and visual observation that the luminescence observed during the automated measurements came from the saponite clots. We suggest that impurities in the saponite on the exterior surface might be the source of the high luminescent background. Only on the weathered surface was a trace of quartz observed; it is likely an interloper mineral deposited by a sedimentary process. A trace of anatase was observed on the freshly cut surface, and a trace was also found on the weathered surface, but none was found during the automated grid measurements.

The ratio of hematite to pyroxene is roughly the same for both surfaces: 1.34 for the weathered surface and 1.50 for the freshly cut surface. The ratio of hematite to plagioclase, however, is a factor of 2 higher in the weathered surface (3.1 compared with 1.8), and thus the ratio of pyroxene to plagioclase on the weathered surface is also higher than on the freshly cut surface (2.3 to

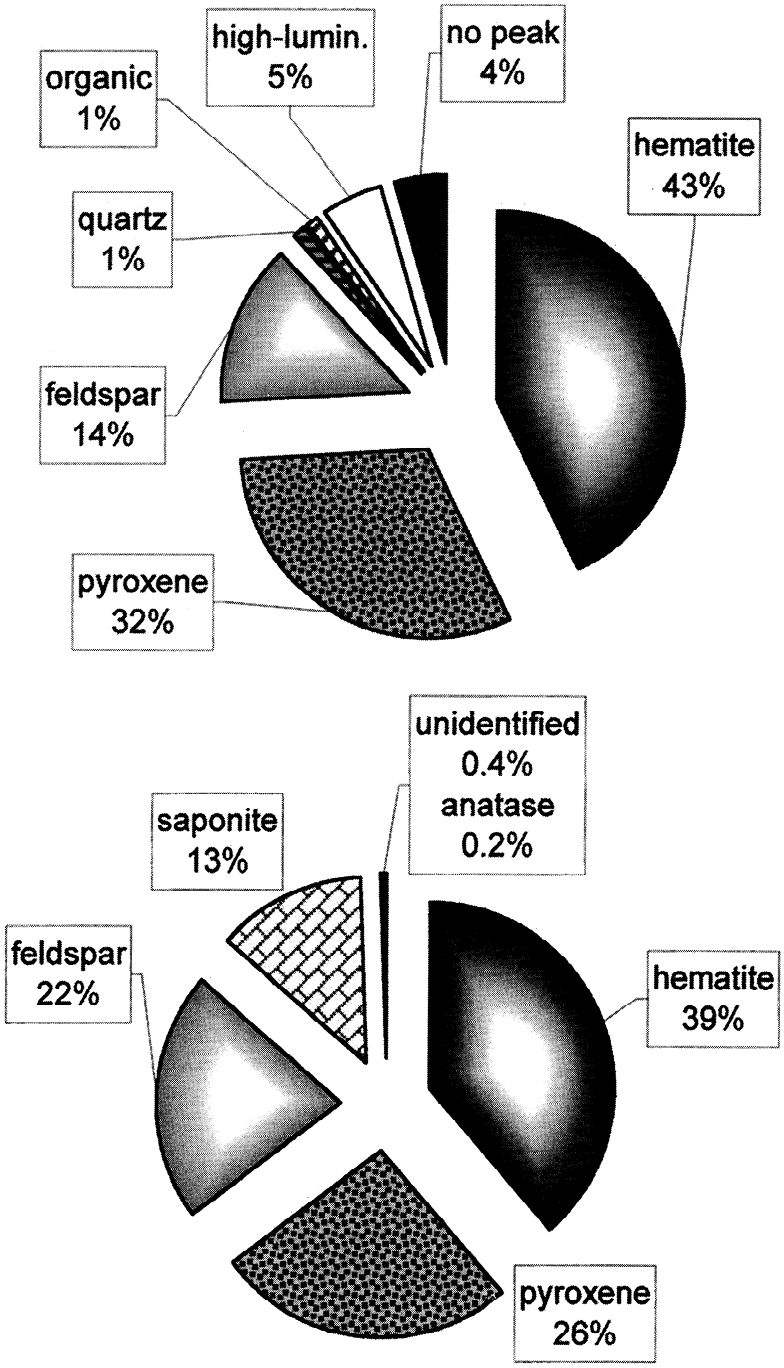

Figure 4. Mineral modes of the rock matrix obtained from the point-counting measurements on the rectangular grid areas (a) on the heavily weathered exterior surface of the rock and (b) on the roughly cut, flat, unpolished interior surface of the rock.

1.2). This confirms that mineral modes obtained on altered rock surfaces require careful interpretation.

Because we have the specimen of weathered basalt in hand and we know where it came from, we know that it was originally a basalt. We can speculate reasonably on petrologic grounds that the saponite is an alteration product of olivine, although no residual olivine was found by petrographic examination of a thin section of the rock. We can estimate the mineral proportions only roughly from the Raman spectra because the hematite is so ubiquitous and, being a strong Raman scatterer, dominates so many of the spectra. We can estimate the pyroxene to plagioclase ratio only very roughly (given the state of alteration or original pyroxene and plagioclase), as about 1.2 to 2.3. Much of what used to be plagioclase is now a mixture of zeolite and alkali feldspar, and much of the pyroxene is oxidized and coated by hematite, and possibly altered in such a way as to no longer give pyroxene spectra useful for determining Mg'.

Although we have reported the results as modes in Figure 4, these results are not the modes that one would obtain by petrographic point counting. Obviously, given the small number of points, the statistical uncertainty would be relatively high, and we do not offer a statistical treatment (as is routinely done, using the

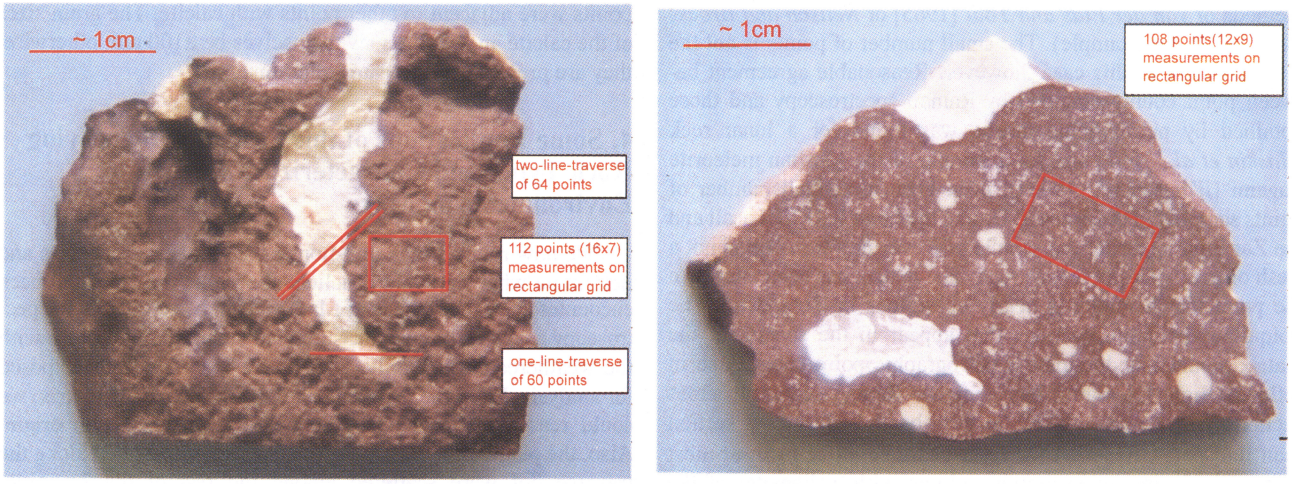

Plate 1. Samples of altered Keweenawan basalt AKB-1: (a) the sample of the weathered rock surface and (b) the roughly sawn flat surface.

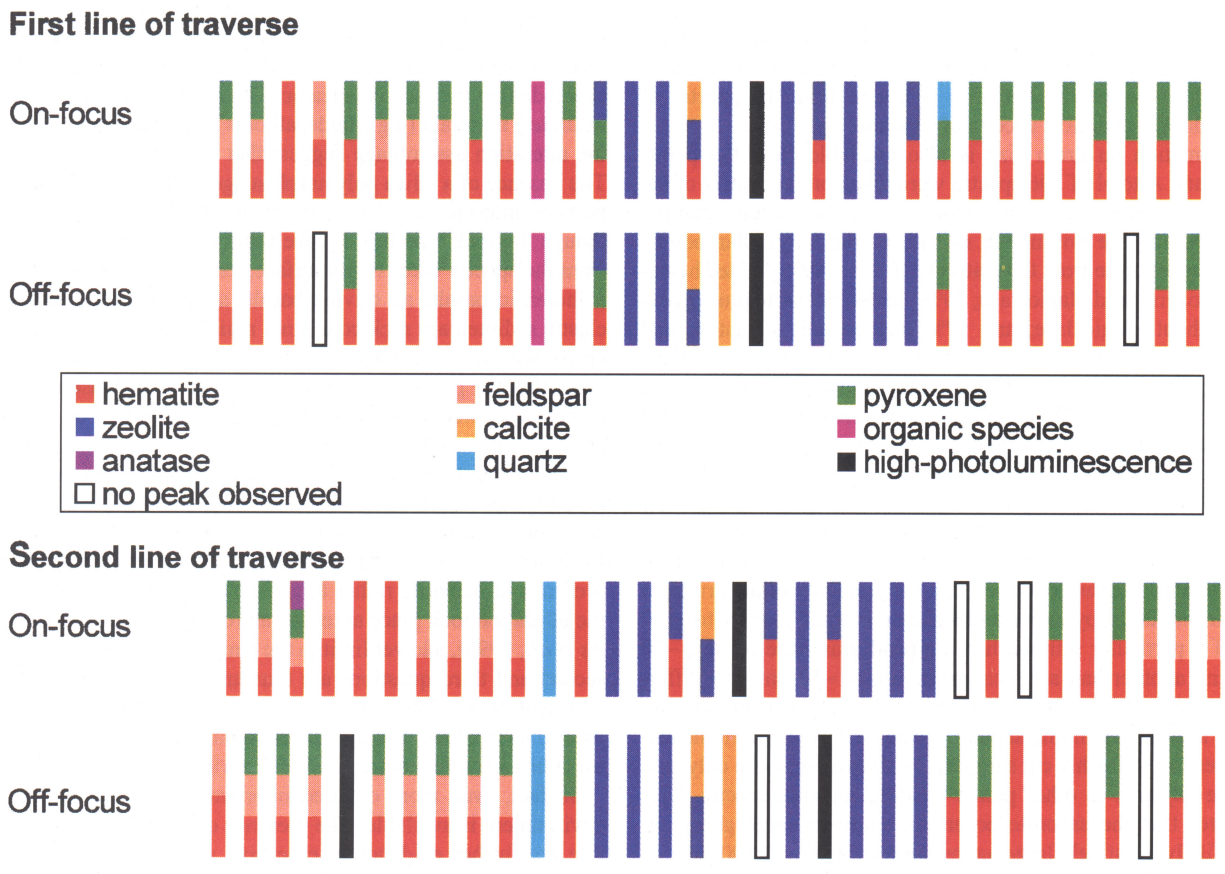

Plate 2. Mineral phase distributions along a two-line traverse on the weathered exterior surface of the AKB-1 (see Plate 1a). The results obtained by on-focus and off-focus (using the automated stage) point-count measurements at the same spots are compared.

methods of *van der Plas and Tobi* [1965] or *Neilson and Brockman* [1977], for example). The small number of points is not the main problem in this case, however. Reasonable agreement between point counts obtained by Raman spectroscopy and those obtained by petrographic means was found for a lunar rock [*Haskin et al.*, 1997] and for a sample of the Martian meteorite Zagami [*Wang et al.*, 1999a], even given the small number of points sampled in those cases. Unlike the lunar KREEP basalt and the Zagami meteorite, the sample of Keweenawan basalt is not a fresh or nearly fresh igneous rock. The matrix has been altered to the point that hematite is nearly ubiquitous in the spectra. The ubiquitous hematite coatings that appear in the spectra of the matrix would not dominate a petrographic point count done in reflected light. Hematite has a higher Raman scattering cross section than pyroxene, which in turn, has a higher cross section than feldspar. Given that the laser beam is out of focus at most points, producing an excitation volume with a diameter of the order of ~100 μm, hematite appears in the spectra even when that mineral occupies a minor part of the laser excitation volume. Also, the farther out of focus the laser beam is, the more likely it is that hematite will dominate the spectrum and the less likely it is that the less sensitive pyroxene and, especially, feldspar will appear. The igneous minerals of the rock were identified readily and unambiguously by this experiment, but their relative proportions could not be obtained accurately. It will be necessary to study rocks at different stages of alteration to learn how to interpret their spectra and determine how best to do quantitative mineralogy and how well igneous mineralogy can be reconstructed. In contrast to the matrix, hematite is absent from the spectra of amygdular fill and most spectra of saponite.

Information on grain size is also available from the point-count data. A total of 306 spectra were taken on the matrix of the two AKB-1 samples (not including the saponite-containing points, which are within the matrix, or the amygdular points, which are separate from the matrix). Of these, 49% yielded hematite, pyroxene, and plagioclase; 29% yielded hematite plus pyroxene without plagioclase; and 17% yielded only hematite, and most of these had a low signal-to-noise ratio. Only 5% of the matrix points yielded hematite plus plagioclase without pyroxene, and only 1 point yielded plagioclase plus pyroxene without hematite. This indicates that the matrix is fine-grained enough that the sampling volumes in our Raman experiments, which have diameters ≤100 μm consistently intercepted several grains and usually intercepted grains of both plagioclase and pyroxene plus hematite alteration products (whether the beam was in focus or out of focus, Plate 2). We thus conclude that the grain size of the principal igneous minerals, pyroxene and feldspar, is small relative to ~100 μm. If a particular mineral had a typical grain size of, say, ~10 μm, and another had a typical grain size of ~50 μm, this difference would not have been detected by this experiment. Also, of the 16 spectra containing saponite peaks (all were within the matrix area of the freshly cut sample), 11 showed saponite only, and 5 were adjacent to other points yielding saponite spectra. This indicates that the saponite occurs as relatively large grains or, more likely, relatively large aggregations of grains (≥100 μm).

Most of the 52 points taken on amygdular material showed peaks for only a single mineral. Forty of these points yielded zeolite spectra, and of these, 29 were of zeolite only. Fifteen of these zeolite spectra were adjacent to another point yielding a zeolite spectrum, indicating that the amygdules are relatively large (hundreds of μm; see also Plate 2). Only four points that yielded zeolite also yielded calcite. Twelve points yielded calcite spectra, six of these yielded calcite spectra only, and three of the points were adjacent to other points with calcite. The grain sizes of the calcite and zeolite may themselves be ≥100 μm; otherwise, they are present as aggregates of grains.

4. Some Implications of this Study for Identifying Rock Types and Characterizing Past Environments on Mars

We now return to the questions asked in the introduction and determine what we could conclude about this rock if it had been encountered on the surface of Mars and analyzed by Raman spectroscopy as a stand-alone measurement technique. We begin with the weathered surface only, as if no fresh surface were exposed for analysis. From the pyroxene and plagioclase of the matrix, we could reasonably conclude that the rock is igneous in origin. Also, the plagioclase-bearing spectra were not clustered along the traverse but were scattered among the rest of the Fe-oxide-dominated spectra, most of which also included a peak for pyroxene. Thus it would be plausible to conclude that the Fe oxides represented the weathering product of pyroxene intimately mixed with plagioclase. From the roughly subequal proportions of those minerals, we could conclude that the igneous rock was mafic. Knowing that plagioclase is a weaker Raman scatterer than either pyroxene or hematite, and that most measurement points were not in good optical focus so that the exciting laser beam was spread onto an area perhaps 100 μm in diameter, we would suspect that the observed proportion of plagioclase was less than the true rock mode. Given that and the relatively small grain size, we would conclude that the rock is volcanic. The absence of primary undersaturated minerals (e.g., feldspathoids) and the calcic nature of the alteration assemblage suggest that the lava was not alkalic. The absence of a silica polymorph suggests the lava was mafic or perhaps intermediate. Thus, in answer to the first question, although the rock type in this case cannot be determined precisely from the spectra taken on its surface, its identity can be limited to a tholeiitic basalt, an olivine basalt, an andesite, or possibly a clastic sedimentary rock consisting mainly of those igneous minerals. We would tentatively rule out a clastic sediment on the basis that the proportions of pyroxene and plagioclase appear to be roughly cotectic, once their relative sensitivities of detection are taken into account.

Because virtually all of the pyroxene spectra occurred in multimineral spectra dominated by hematite, we would infer that the hematite was a derivative of the pyroxene and had been produced by weathering or alteration in an oxidizing environment. The presence of hematite rather than Fe-oxyhydroxides suggests that the alteration took place at temperatures above 250–300°C [*Morris et al.*, 1995], a lower limit to the temperature of alteration. The second and third questions are thus answered: The environment was hydrothermal and probably subsurface, and it was oxidizing as well as aqueous, and this information was obtained from spectra obtained on the unprepared rock surface.

In fact, even more detailed information about the alteration environment is available. The presence of the calcite and thomsonite are further evidence of extensive alteration. The extensive concentration of calcite and zeolite in a single location as observed on a linear traverse would indicate filling of a vein or an amygdule. (The Raman experiment on Mars could presumably be targeted to cross such a macroscopic feature through prior observation by the imaging camera required to guide a rover or a lander arm to a sample for analysis. In a sophisticated mission with a close-up microscopic imager, such targeting should be routine.) Generally speaking, calcite could be low-temperature sedimen-

tary, higher-temperature hydrothermal, or even igneous in origin. Thomsonite, containing waters of hydration, may be stable to relatively high temperatures for a zeolite but not to greater than about 350 °C [*Miyashiro and Shido*, 1970], providing an upper limit to the temperature of alteration. The presence of the specific zeolite thomsonite would enable us to distinguish hydrothermal alteration that might have occurred at depth in the Martian crust, from acid-sulfate weathering that might have been associated with volcanic activity at the surface. *Ming and Gooding* [1988] indicate that only the most siliceous zeolites (Si>>Al atomic) are expected to be stable in an acid-sulfate environment.

Suppose we were fortunate enough to identify the saponite. This might be possible because of a different regime of surface alteration on Mars in which the saponite was not all photoluminescent, perhaps because sandblasting refreshed weathered surfaces without scouring the soft clays or because there were drill cores or cuttings available for Raman analysis. The presence of saponite could result from surface weathering or from hydrothermal alteration. The stability of saponite implies temperatures no greater than ~ 500°C [*Morris et al.*, 1995], although we would expect loss of interlayer water in the interval of 100–250°C and progressive loss of OH beyond 300°C. The identification of large grains or aggregates of pure saponite, a highly magnesian clay mineral, would be consistent with alteration of olivine phenocrysts. (Olivine is expected to be the least stable of the original igneous minerals under alteration conditions.)

In answer to the final question, in this case, organic carbon was clearly present and it still carried definitive evidence about organic functional groups. The appearance of such an organic Raman spectra obtained during a rover traverse on Mars would surely excite outrageous speculation by some scientists and cause deep suspicion about premission decontamination in others.

Acknowledgments. We thank James Maniotis for identifying the organism as a crustose lichen. We appreciate the identification of the organic functional groups by John Freeman. We gratefully acknowledge a helpful review of the manuscript by H. McSween. This work was supported in part by the National Aeronautics and Space Administration through grant NAG 5-7140.

References

Bell, J. F., III, T. L. Roush, and R. V. Morris, Mid-infrared transmission spectra of crystalline and nanophase iron oxides/oxyhydroxides and implications for remote sensing of Mars, *J. Geophys. Res., 100*, 5297–5307, 1995.

Brannon, J. C., Geochemistry of successive lava flows of the Keweenawan North Shore Volcanic Group, Ph.D. dissertation, 312 pp., Washington Univ., St. Louis, Mo., 1984.

Buseck, P. R., G. L. Nord Jr., and D. R. Veblen, Subsolidus phenomena in pyroxenes, in *Pyroxenes*, edited by C. T. Prewitt, *Rev. Mineral., 7*, 117-211, 1982.

Dutta, P.K., and B. Del Braco, Raman spectroscopic studies of zeolite framework, hydrated zeolite A and the influence of cation, *J. Phys. Chem., 89*, 1861-1865, 1985.

Dutta, P.K., and M. Puri, Synthesis and structure of zeolite ZSM-5: A Raman spectroscopic study, *J. Phys. Chem., 91*, 4329-4333, 1987.

Dutta, P.K., and D. C. Shieh, Crystallization of zeolite: A spectroscopic study, *J. Phys. Chem., 90*, 2331-2334, 1986.

Gottardi, G., Mineralogy and crystal chemistry of zeolites, in *Natural Zeolites: Occurrence, Properties, Use*, edited by L. B. Sand and F. A. Mumpton, pp. 31–44. Pergamon, Tarrytown, N.Y., 1978.

Haskin, L. A., A. Wang, K. M. Rockow, B. L. Jolliff, R. L. Korotev, and K. M. Viskupic, Raman spectroscopy for mineral identification and quantification for in situ planetary surface analysis: A point count method, *J. Geophys. Res., 102*, 19,293–19,306, 1997.

Herman, R. G., C. E. Bogdan, A. J. Sommer, and D. R. Simpson, Discrimination among carbonate minerals by Raman spectroscopy using the laser microprobe, *Appl. Spectrosc., 41*, 437-440, 1987.

Israel, E. J., R. E. Arvidson, A. Wang, J. D. Pasteris, and B. L. Jolliff, Laser Raman spectroscopy of vanished basalt and implications for in situ measurements of Martian rocks, *J. Geophys. Res., 102*, 28,705-28,716, 1997.

Lane, M. D. , R. V. Morris , and P. R. Christensen, An extensive deposit of crystalline hematite in Terra Meridiani, Mars, *Lunar Planet. Sci.* [CD-ROM], *XXX*, abstract 1469, 1999.

McSween, H. Y., Jr., et al., Chemical, multispectral, and textural constraints on the composition and origin of rocks at the mars Pathfinder landing site, *J. Geophys. Res., 104*, 8679–8715, 1999.

Ming, D. W., and J. L. Gooding, Zeolites on Mars: Possible environmental indicators in soils and sediments, in *Workshop on Mars Sample Return Science, LPI Tech. Rep., 88-07*, 124–125, 1988.

Miyashiro, A., and F. Shido, Progressive metamorphism in zeolite assemblages,. *Lithos, 3*, 251–260, 1970.

Morris, R. V., D. C. Golden, J. F. Bell III, and H. V. Lauer Jr., Hematite, pyroxene, and phyllosilicates on Mars: Implications from oxidized impact melt rocks from Manicouagan Crater, Quebec, Canada, *J. Geophys. Res., 100*, 5319–5328, 1995.

Morris, R. V., et al., Analyses of martian surface materials during the Mars Surveyor 2001 mission by the Athena instrument payload, *Lunar and Planet. Sci.*, [CD-ROM], XXIX, abstract 1326, 1998.

Neilson, J., and G. F. Brockman, The error associated with point-counting, *Am. Mineral., 62*, 1238-1244, 1977.

Pechar, F., and D. Rykl, Study of the vibrational spectra of natural natrolite, *Can. Mineral., 21*, 689-695, 1983.

Reider, R., T. Economou, H. Wänke, A. Turkevich, J. Crisp, J. Brükner, G. Dreibus, and H. Y. McSween Jr., The chemical composition of martian soil and rocks returned by the mobile alpha proton X-ray spectrometer: Preliminary results from the X-ray mode, *Science, 278*, 1771-1774, 1997.

Sharma, S.K., B. Simons, and H. S. Yoder Jr., Raman study of anorthite, calcium, Tschermak's pyroxene, and gehlenite in crystalline and glassy states, *Am. Mineral., 68*, 1113-1125, 1983.

van der Plas, L., and A. C. Tobi, A chart for judging the reliability of point counting results, *Am. J. Sci., 263*, 78-90, 1965.

Wang, A., Some grain size effects on Raman scattering intensity for in situ measurements on rocks and soils: Experimental tests and modeling, *Lunar and Planet. Sci.* [CD-ROM], *XXX*, abstract 1644, 1999.

Wang, A., J. Han, L. Guo, J. Yu, and P. Zeng, Database of standard Raman spectra of minerals and related inorganic crystals, *Appl. Spectrosc., 48*, 959-968, 1994.

Wang A., B. L. Jolliff, and L. A. Haskin, Raman spectroscopy as a method for mineral identification on lunar robotic exploration missions, *J. Geophys. Res., 100*, 21,189–21,199, 1995.

Wang, A., L. A. Haskin, and E. Cortez, A Raman sensor for in situ mineral characterization on planetary surfaces, *Appl. Spectros., 52*, 477-487, 1998a.

Wang, A., L. A. Haskin, and B. Jolliff, Characterization of mineral products of oxidation and hydration by Raman spectroscopy -- Implication for in situ petrologic investigation on the surface of Mars, *Lunar Planetary Sci.*, [CD-ROM], *XXIX*, abstract 1819, 1998b.

Wang, A., B. L. Jolliff, and L. A. Haskin, Raman spectroscopic characterization of a Martian SNC meteorite: Zagami, *J. Geophys. Res., 104*, 8509-8519, 1999a.

Wang, A., B. L. Jolliff, L. A. Haskin, and K. E. Kuebler, Raman spectral features of pyroxene – Application to Martian meteorites Zagami and EETA79001, *Lunar Planet. Sci.*, [CD-ROM], *XXX*, abstract 1666, 1999b.

Wopenka, B., J. J. Freeman, and T. Nikischer, Raman spectroscopic identification of fibrous natural zeolite, *Appl. Spectrosc., 52*, 54-63, 1998.

L. A. Haskin, B. L. Jolliff, and A. Wang, Department of Earth and Planetary Sciences, Campus Box 1169, Washington University, One Brooking Drive, St. Louis, MO 63130-4899. (alianw@levee.wustl.edu)

(Received April 20, 1999; revised July 27, 1999; accepted July 30, 1999.)